**Cell Metabolism, Volume *19***

## Supplemental Information

# Endothelial PGC-1α Mediates Vascular Dysfunction in Diabetes

**Naoki Sawada, Aihua Jiang, Fumihiko Takizawa, Adeel Safdar, Andre Manika, Yevgenia Tesmenitsky, Kyu-Tae Kang, Joyce Bischoff, Hermann Kalwa, Juliano L. Sartoretto, Yasutomi Kamei, Laura E. Benjamin, Hirotaka Watada, Yoshihiro Ogawa, Yasutomi Higashikuni, Chase W. Kessinger, Farouc A. Jaffer, Thomas Michel, Masataka Sata, Kevin Croce, Rica Tanaka, and Zolt Arany**

# Inventory of Supplemental Information

## Supplemental Data

**Movie S1**, Related to Figure 2
**Movie S2**, Related to Figure 2

**Figure S1**, Related to Figure 1
**Figure S2**, Related to Figure 2
**Figure S3**, Related to Figure 3
**Figure S4**, Related to Figure 4
**Figure S5**, Related to Figure 5
**Figure S6**, Related to Figure 6

**Table S1**, Related to Figure 1
**Table S2**, Related to Figure 1

## Supplemental Experimental Procedure

## Supplemental References

# Supplemental Data

**Movies S1 and S2. Endothelial PGC-1α inhibits cell migration in vivo, Related to Figure 2.**
Time-lapse videoscopy of scratch assays performed with control HUVECs (**Movie S1**) vs. HUVECs overexpressing PGC-1α (**Movie S2**) demonstrates that the latter remains capable of small-distance random vibration, but fails to undergo directional cell movement.

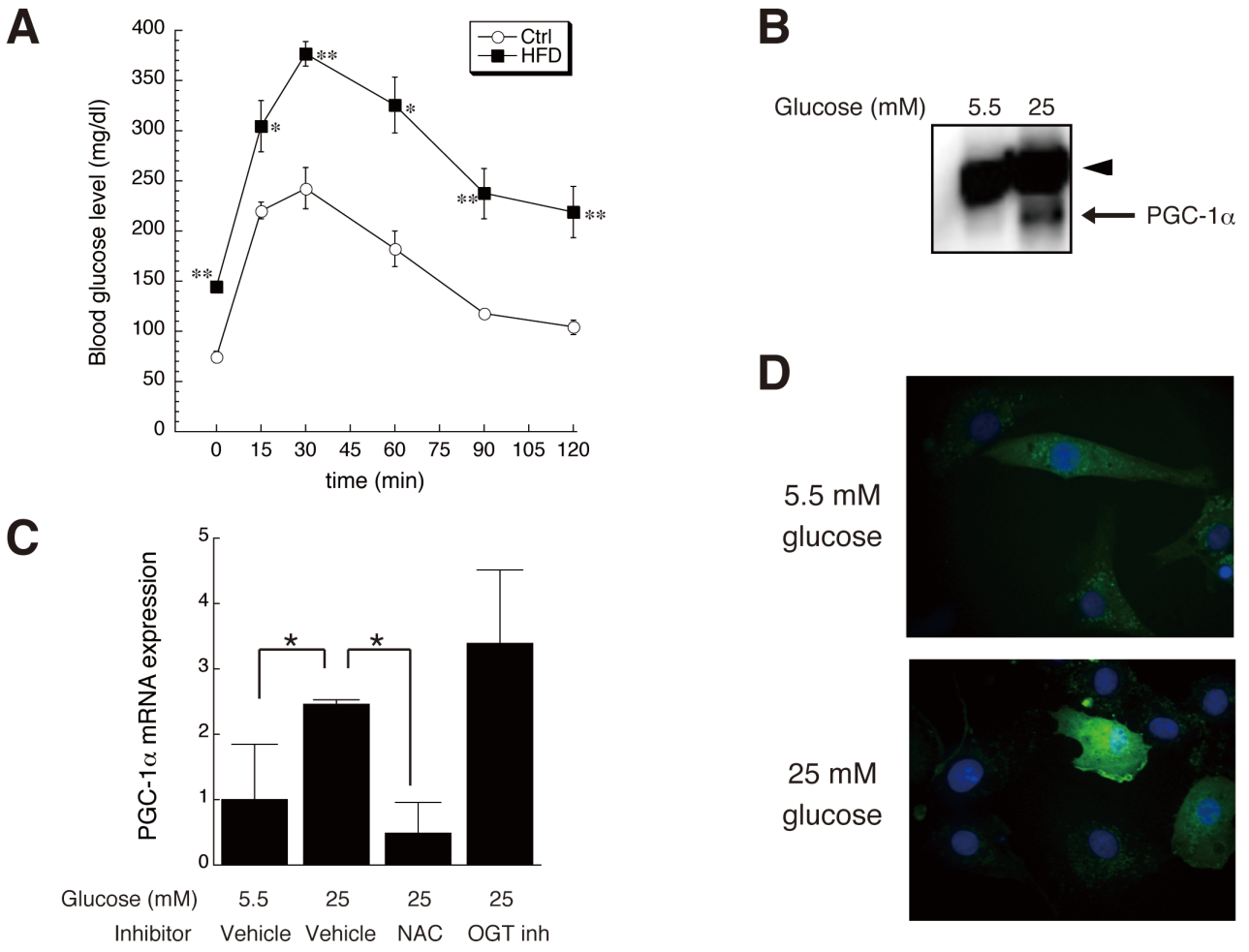


**Figure S1, Related to Figure 1.**
(A) Glucose tolerance test, demonstrating the induction of type II diabetes in mice fed a high-fat diet (HFD). (B) Immunoprecipitation (IP)-western blotting, showing up-regulation of PGC-1α protein expression by high glucose treatment (25 mM) of cultured mouse muscle endothelial cells (MMECs). IP was conducted with a rabbit polyclonal anti-PGC-1 antibody (H-300, Santa Cruz) and immunoblotting was perofrmed using mouse monoclonal anti-PGC-1α antibody (Calbiochem, 4C1.3). Arrowhead, internal loading control (non-specific bands). (C) Glucose induction of PGC-1α mRNA expression in mouse heart ECs (MHECs) is mediated by reactive oxygen species (ROS), but not by glucose-mediated glycosylation. Vehicle, 0.068% DMSO. NAC, N-acetyl cysteine (1 mM). OGT (O-GlcNAc Transferase) inhibitor, Benzyl-2-acetamido-2-deoxy-α-D-galactopyranoside (1 mM). (D) Increased ROS in BAECs treated with high glucose, visualized in green by hydrogen peroxide biosensor, HyPer2. N = 4 for each group. Data are means ± SEM. *, $P < 0.05$. **, $P < 0.01$.

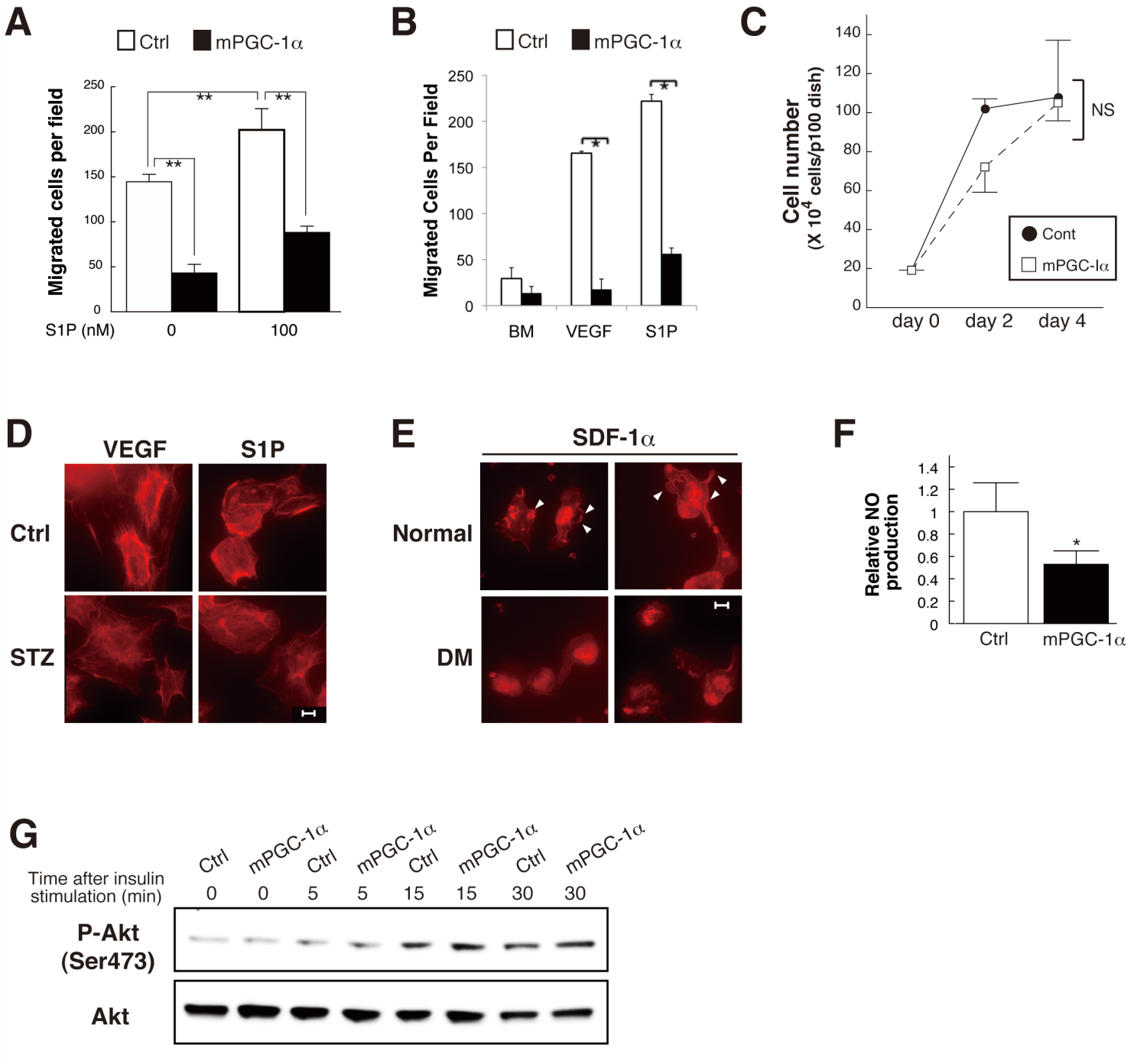


**Figure S2, Related to Figure 2.**

(A–C) Retroviral overepression of mouse PGC-1α in MMECs (A), human ECFCs (B) and HUVECs (C) diminishes the migratory capacity in Transwell assay (A, B), but does not affect cell proliferation (C). (D and E) Pro-migratory stimuli-induced lamellipodia formation and subcortical F-actin accumulation (arrow heads), visualized by Alexa546-labeled phalloidin staining, are impaired in MLECs from STZ-treated mice (D) and EPCs from diabetic patients (E). Scale bars, 20 $\mu$m. (F) DAF-2 fluorescence assessment of cell culture supernatant reveals reduced NO production after 1hr VEGF stimulation in HUVECs retrovirally transduced with mouse PGC-1α. (G) No effect of PGC-1α overexpression in HUVECs on 10 $\mu$g/ml insulin-induced Akt phosphorylation. N = 3-9 per group. *, $P < 0.05$. **, $P < 0.01$. Data are means ± SEM.

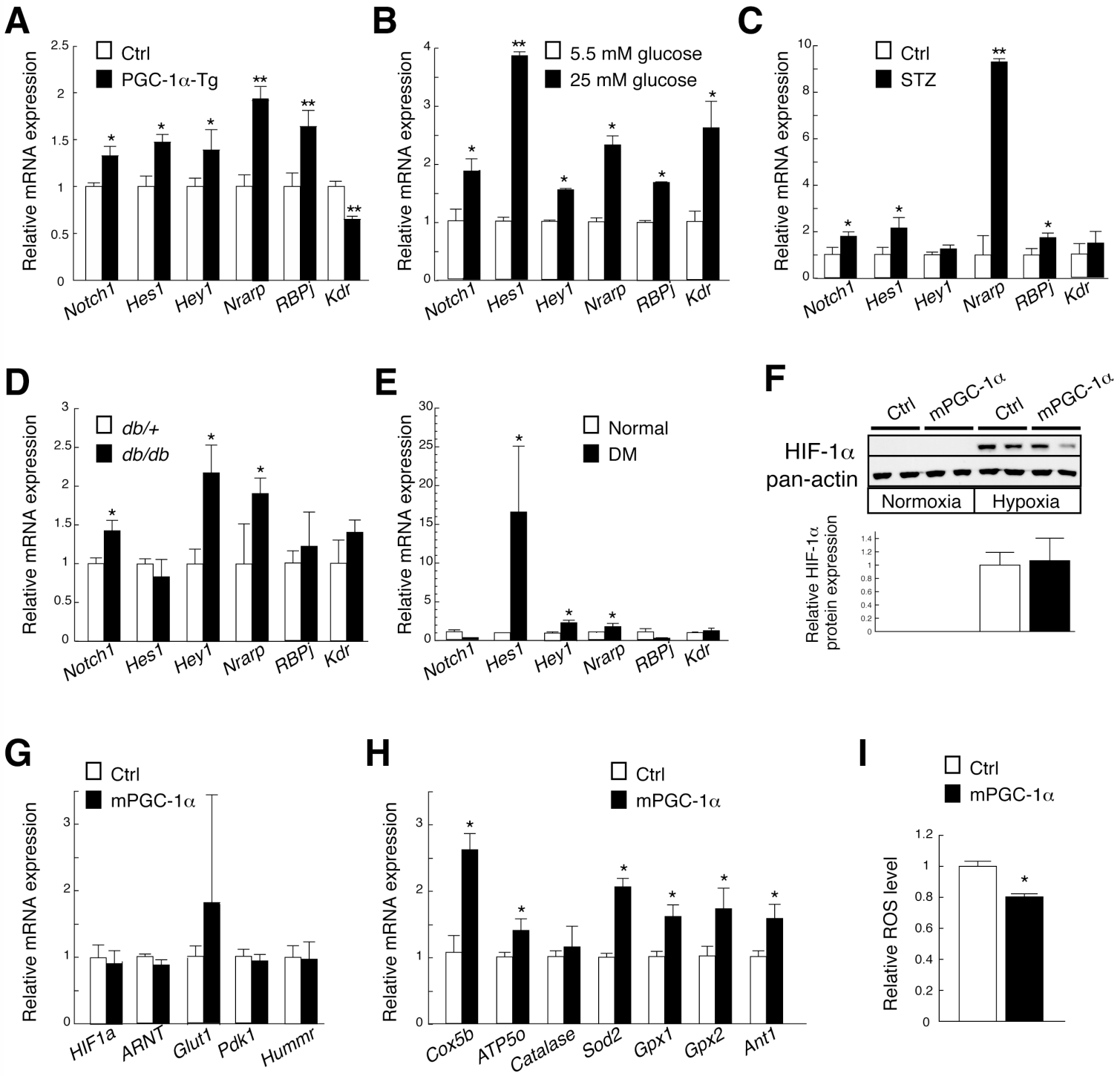


**Figure S3, Related to Figure 3.**

(A–E) Augmented mRNA expression signature of Notch activation in cultured MMECs isolated from EC-PGC-1α-Tg mice (A), human dermal microvascular ECs treated with high glucose for 24 hours (B), mouse lung ECs (MLECs) isolated from STZ-treated type 1 diabetic mice (C), the EC compartment of *db/db* mouse skeletal muscle (D), and cultured EPCs isolated from type 2 diabetic patient peripheral blood (E). (F) HIF-1α protein expression in HUVECs, both under normoxic and hypoxic conditions, is not affected by retrovirus-mediated forced expression of PGC-1α. (G) mRNA expession of HIFs and their target genes is not altered by forced expression of PGC-1α in HUVECs. (H) mRNA expression of mitochondrial ROS detoxification system genes is mildly increased by over-expression of PGC-1α in HUVECs. (I) Cellular ROS level as assessed by DCF fluorescence is mildly suppressed by over-expression of PGC-1α in HUVECs. N = 3 per group. *, $P < 0.05$. **, $P < 0.01$. Data are means ± SEM.

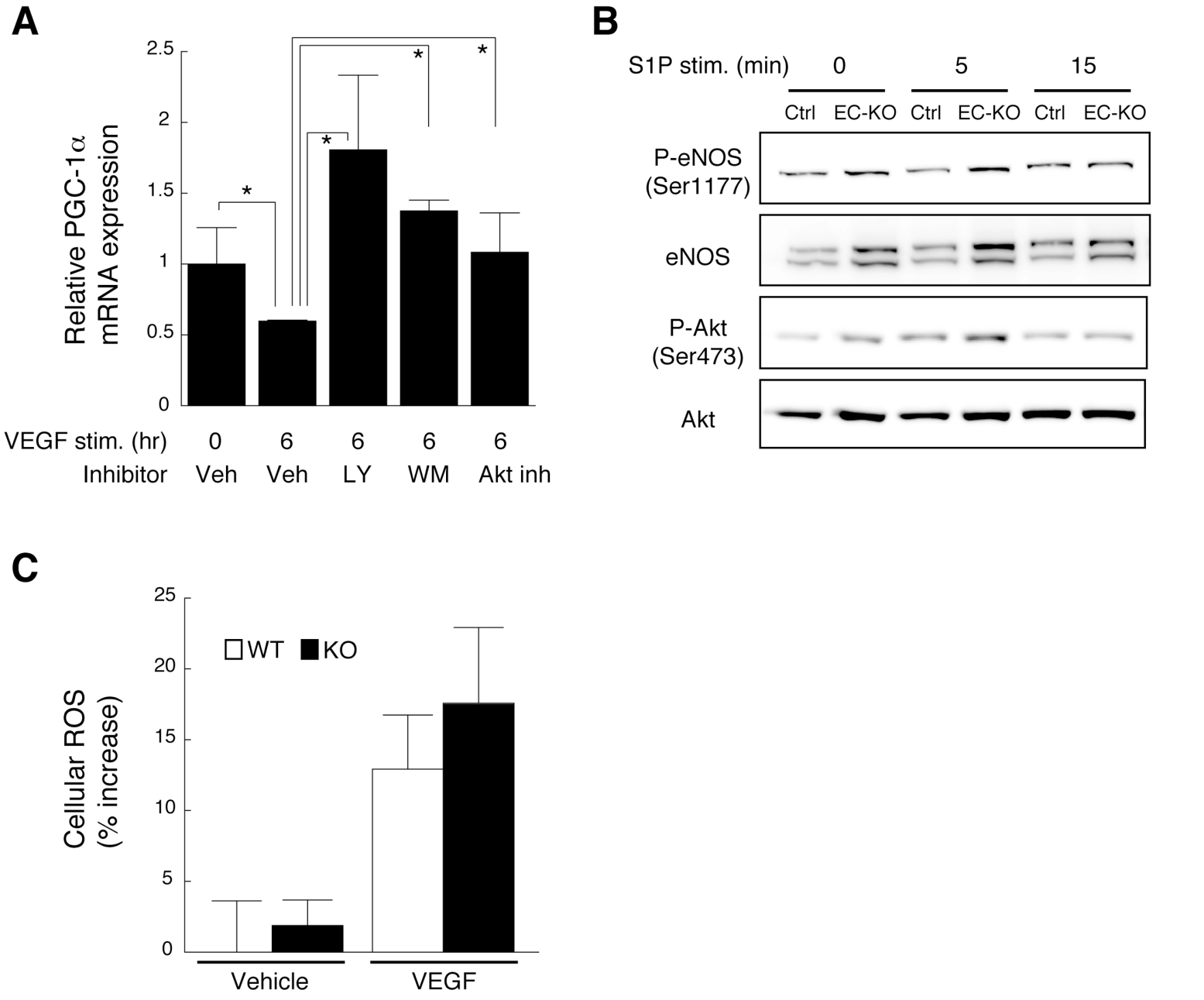


**Figure S4, Related to Figure 4.**

(A) VEGF-induced downregulation of PGC-1α mRNA expression is mediated by PI-3 kinase and Akt. Human dermal microvascular ECs were stimulated with 10 ng/mL VEGF for 6 hours in the presence of either vehicle (0.05% DMSO, Veh), 5 $\mu$M LY 294002 (LY), 0.5$\mu$M Wortmannin (WM), or 5 $\mu$M Akt Inhibitor IV (Akt inh). (B) Enhanced phosphorylation of eNOS and Akt by 100 nM S1P in the MMECs from EC-specific PGC-1α KO mice. (C) No difference between PGC-1α null and wild-type MHECs in cellular ROS level as assessed by DCF fluorescence, without or with 30-min stimulation by 10 ng/mL VEGF. N = 3–6 per group. *, $P < 0.05$. Data are means ± SEM.

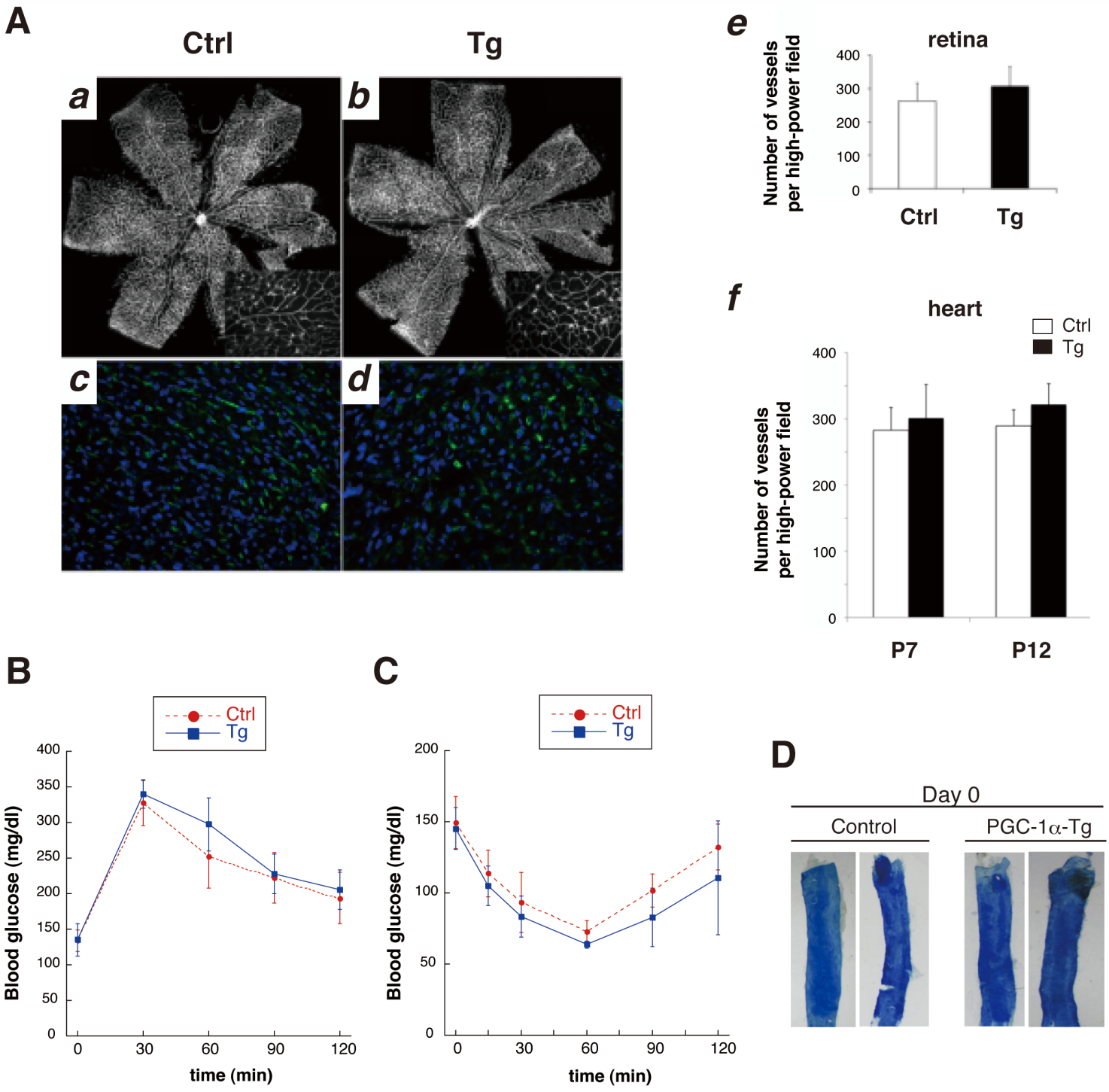


**Figure S5. Forced expression of PGC-1α in transgenic mouse endothelium does not affect basal vascular development, systemic glucose handling, blood pressure, systemic vascular resistance, nor baseline blood flow in vivo but diminshes re-endothelialization of injured vessels, skin wound healing, increase of blood flow in response to acteylcholine, and endothelium-dependent vasorelaxation. Related to Figure 5.**

(A) Left, representative retinal vascular images and immunostainig (CD31 (green) and DAPI (blue)) for control (a and c) and PGC-1α Tg mice (Tet-Off, b and d). Right, quantification of vacular density in retina (e) and the heart (f) from P7 and P12 pups. (B and C) Glucose tolerance test (B) and insulin tolerance test (C) of PGC-1α Tg mice (Tet-On). (D) Day 0 images of the control and PGC-1α-Tg mouse (Tet-Off) carotid arteries (luminal side) following catheter-mediated injury, with denudaded areas visualized by Evans Blue staining.

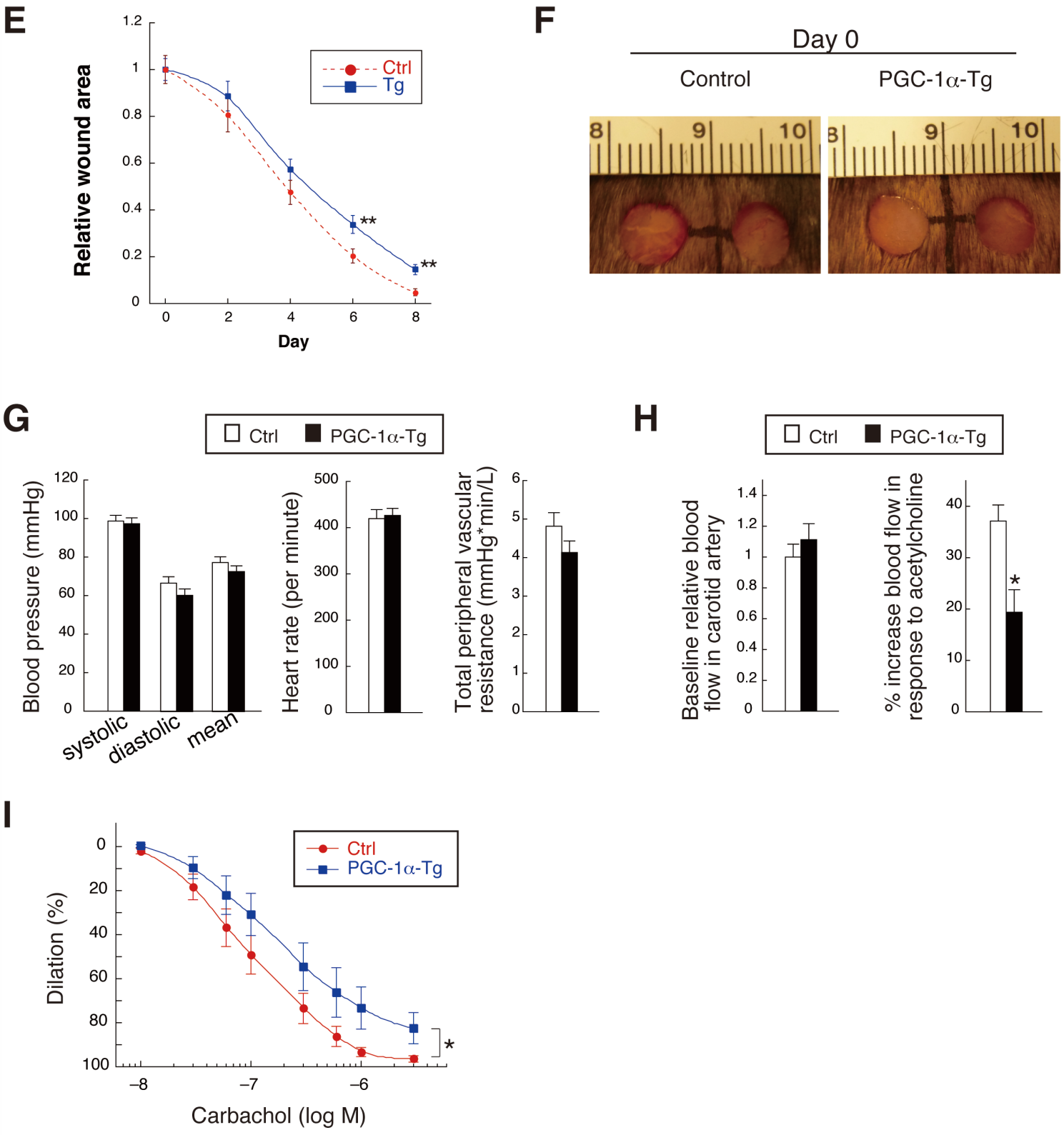


**Figure S5 (continued).**

(E) Skin wound healing of PGC-1α Tg mice (Tet-On). (F) Day 0 images of the control and PGC-1α-Tg mouse (Tet-Off) back skin following the creation of wounds by skin punching. (G) Arterial blood pressure, heat rate, and systemic vascular resistance of control and PGC-1α-Tg mice (Tet-On). (H) Carotid artery blood flow in intact control and PGC-1α-Tg mice (Tet-Off). (I) Carbachol-induced dilation of carotid artery explants isolated from control and PGC-1α-Tg mice (Tet-Off). N = 3-10 for all groups. *, $P < 0.05$. **, $P < 0.01$. Data are means ± SEM.

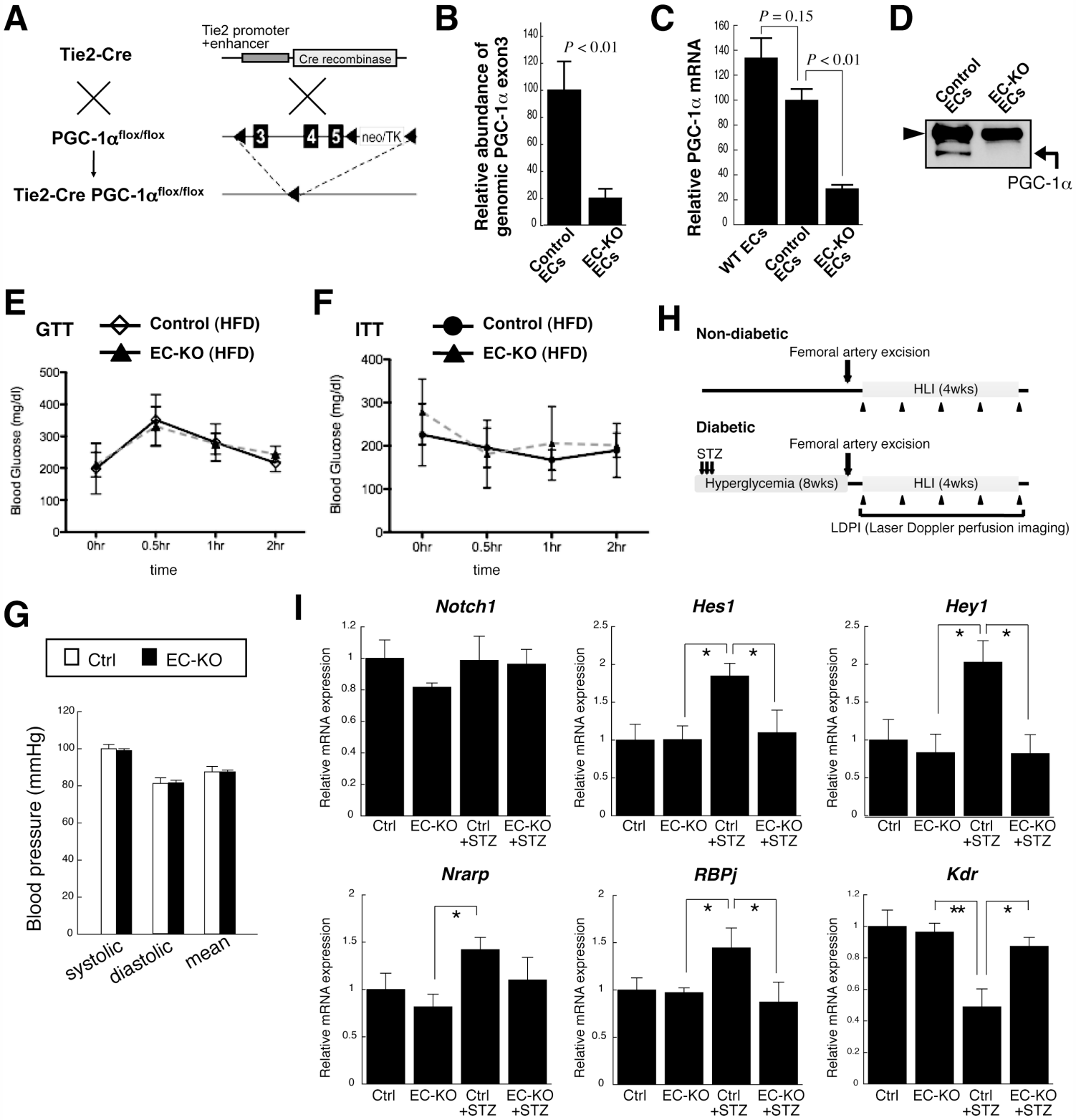


**Figure S6. Generation of endothelial-specific PGC-1α knockout mice (EC-KO). Related to Figure 6.**

(A) Schema showing the development of EC-KO mice. (B-D) Genomic index showing ~80% deletion of the PGC-1α gene exon 3 (B) and PGC-1α mRNA expression decreased by ~70% (C) in EC-KO MLECs compared to control. Immunoprecipitation-western blot showing the absence of PGC-1α protein expression in EC-KO MMECs (D). Arrowhead, internal loading control (non-specific bands). (E and F) Systemic glucose handling is not altered in EC-KO mice, as assessed by glucose tolerance test (E) and insulin tolerance test (F). (G) No difference in blood pressure, as assessed by the tail cuff method, between control and EC-KO mice. (H) Schema showing the induction of hyperglycemia by STZ in mice, followed by hind-limb ischemia through femoral artery excision. (I) EC-KO and control mice were left euglycemic or rendered hyperglycemic for 8 weeks as depicted in F. The lung endothelial fraction was freshly harvested to assess mRNA expression of the Notch pathway genes. N = 3-10 per group. *, $P < 0.05$. **, $P < 0.01$. Data are means ± SEM.

**Table S1. Clinical characteristics of mouse models. Related to Figure 1.**

| Mouse models | | AST (GOT) (IU/L) | Free fatty acids (μEq/L) | Glucose (mg/dl) | Triglyceride (mg/dl) | Total Cholesterol (mg/dl) |
|---|---|---|---|---|---|---|
| **STZ-induced diabetic mice** | | | | | | |
| (N = 8) | Ctrl | 70 ± 4 | 386 ± 46 | 232 ± 7 | 11 ± 1 | 53 ± 3 |
| | STZ | 85 ± 8 | 564 ± 70 | 479 ± 52 | 22 ± 4 | 65 ± 5 |
| ***ob/ob* mice** | | | | | | |
| (N = 4) | +/+ | 89 ± 6 | 483 ± 68 | 221 ± 4 | 37 ± 7 | 71 ± 2 |
| | *ob/ob* | 195 ± 34 | 505 ± 66 | 309 ± 12 | 10 ± 1 | 147 ± 6 |
| ***db/db* mice** | | | | | | |
| (N = 4) | *db/+* | 75 ± 9 | 463 ± 29 | 167 ± 16 | 53 ± 7 | 71 ± 2 |
| | *db/db* | 93 ± 22 | 773 ± 65 | 620 ± 34 | 117 ± 18 | 149 ± 16 |
| **EC-PGC-1α KO mice** | | | | | | |
| (N = 8–11) | Ctrl | 106 ± 14 | 394 ± 41 | 175 ± 13 | 19 ± 4 | 47 ± 4 |
| | KO | 110 ± 13 | 425 ± 28 | 165 ± 9 | 18 ± 3 | 49 ± 5 |
| **EC-PGC-1α Tg mice (Tet-on)** | | | | | | |
| (N = 8) | Ctrl | 86 ± 9 | 465 ± 47 | 180 ± 12 | 41 ± 14 | 82 ± 6 |
| | Tg | 90 ± 16 | 474 ± 84 | 163 ± 16 | 20 ± 4 | 86 ± 6 |

Data were obtained from plasma collected from mice kept *ad libitum*.

**Table S2. Clinical characteristics of patients. Related to Figure 1.**

| | | Diabetic patients (N = 5) |
|---|---|---|
| Total Cholesterol | (mg/dL) | 173.0 ± 18.8 |
| HDL Cholesterol | (mg/dL) | 48.4 ± 9.3 |
| LDL Cholesterol | (mg/dL) | 97.8 ± 7.4 |
| Triglyceride | (mg/dL) | 106.8 ± 17.5 |
| Uric acid | (mg/dL) | 4.1 ± 0.5 |
| Creatinine | (mg/dL) | 0.7 ± 0.1 |
| AST (GOT) | (IU/L) | 23.8 ± 1.9 |
| ALT (GPT) | (IU/L) | 22.6 ± 5.3 |
| HbA1c | (%) | 6.5 ± 0.4 |

# Supplemental Experimental Procedures

**Mouse and human endothelial cells**

All procedures were performed using protocols approved at the relevant institution by Institutional Review Boards for human studies and Institutional Animal Care and Use Committees. Mouse endothelial cells were isolated from the lung, heart, and skeletal muscle, by sequential affinity selection method using Dynabeads sheep anti-rat IgG (Invitrogen, Carlsbad, CA), anti-PECAM1 antibody (BD Biosciences, San Jose, CA), and anti-ICAM2 antibody (BD Biosciences) as described (Sawada et al., 2009; Sawada et al., 2008). Isolated ECs were either immediately harvested to represent the endothelial compartment of mouse organs, or cultured to passage 2 or 3 for cell migration and other assays. Human umbilical vein (HUVECs) and dermal microvascular endothelial cells (HDMVECs) were purchased from Lonza.

**Isolation of human circulating $CD34^+$ cells (circulating progenitor cells, CPCs) and preparation of human EPCs**

Type 2 diabetic patients of Juntendo University Hospital, Department of Metabolism and Endocrinology, were recruited. Peripheral blood (PB) from healthy volunteers and DM patients were obtained with informed consent under the institutional approval of Clinical Investigation Committee. PB samples (50ml/subject) were drawn into tubes containing EDTA-2Na (Venoject II, Terumo, Tokyo, Japan), diluted with the equal volume of PBS and then separated by density gradient centrifugation (1500 rpm, 30 min) using Histopaque-1077 (Sigma, St. Louis, MO). The PB mononuclear cells (PBMNCs) were collected as the intermediate white layer and suspended with PBS containing 2 mM EDTA (EDTA-PBS). After centrifugation (2000 rpm, 20 min), the cells were treated with $NH_4Cl$ solution (pH 7.3) for 10 min at room temperature for lysing contaminated erythrocytes, and then washed with ETDA-PBS by centrifugation twice. The cells were suspended with EGM-2 medium (Lonza) for the subsequent procedures. The preparation of CD34+ cells was modified from our previous reports for the preparation of CD133+ cells (Masuda et al., 2011; Masuda et al., 2007; Nakamura et al., 2012). In brief, CD34+ cells were isolated from PB-mononuclear cells using CD34 microbeads kit including mirobeads conjugated to monoclonal mouse anti-human CD34 antibody (Miltenyi Biotec, Bergisch Gladbach, Germany) on an AutoMACS separator (Miltenyi). For preparing EPCs, the PBMNCs were seeded at 1 x $10^7$ cells/well on a 6-well Primaria culture plate (BD) with 2 ml of EGM-2 or at 1 x $10^6$ cells/chamber on a 4-chamber slide (Lab-Tek) with 0.5 ml of EGM-2. The media were replaced with fresh media every 3-4 days. The cells were used as EPCs at day 10-14 for following applications.

**Animals**

Age-matched litters (12–20 wk) were used for test and control groups in all experiments. The development of PGC-1α knockout mice was described elsewhere (Lin et al., 2004). PGC-1α conditional allele knock-in mice were developed as described (Handschin et al., 2007), and backcrossed at least eight times onto the C57BL/6 strain. Two strains of Tie2-Cre transgenic mice were used for the study, and yielded essentially similar results. The first line (Flavell)(Koni et al., 2001) was obtained from Jackson Laboratory (Bar Harbor, ME). The second line (Yanagisawa)(Kisanuki et al., 2001) was obtained from Dr. Thomas N. Sato. Endothelial-specific PGC-Iα knockout mice (Tie2-Cre PGC-$1\alpha^{flox/flox}$) were created by crossbreeding of PGC-1α conditional allele knock-in mice with Tie2-Cre mice as depicted in Fig. 4a. In experiments, littermates with Tie2-Cre PGC-$1\alpha^{flox/+}$ genotype were used as a control. Two independent lines of tetracycline-inducible, endothelial-specific PGC-1α transgenic mice were generated, as shown in Fig. 3b. The first line ("Tet-off" mice) was created as double Tg mice by crossing VE-cadherin promoter-driven tetracycline transactivator (tTA) Tg mice (VE-cad-tTA)(Sun et al., 2005) with

tetracycline response element-driven PGC-1α Tg mice (TRE-PGC-Iα)(Russell et al., 2004). TRE-PGC-1α Tg mice are a generous gift from Dr. Dan Kelly. The second line ("Tet-on" mice) was similarly generated by crossing Tie2-promoter/enhancer-driven reverse tetracycline transactivator (rtTA) Tg mice (Tie2-rtTA)(Teng et al., 2002), purchased from the Jackson Laboratory, with TRE-PGC-1α mice. The "Tet off" double Tg mice were administered doxycycline (Dox) in their drinking water (2 mg/ml) supplemented with 5% sucrose, and the gene induction was initiated via the removal of Dox. Conversely, the gene induction in "Tet-on" Tg mice was achieved by administration of the Dox containing drinking water 2 days before the start of the hindlimb ischemia experiment. As a control, littermates with Tie2-rtTA Tg genotype were used.

**Diabetic mouse models**

We used 4 types of diabetic mouse models. (i) Streptozotocin (STZ) model. Type 1 diabetes was induced in C57BL6/J mice via intraperitoneal administration of STZ dissolved in 200 $\mu$l of 10mM sodium citrate buffer, pH 4.0 (70 mg/kg × 3 days). The blood glucose level at ad libitum condition was assessed at day 14. The mice whose blood glucose level exceeded 200 mg/dl were used for experiments. (ii) High fat feeding (HFD). Type 2 diabetes was induced by the conventional model of high fat diet-induced obesity (DIO), using Rodent Diet with 60 kcal% fat (cat# D12492, Research Diets Inc., New Brunswick, NJ). HFD feeding was conducted with C57BL/6J mice for 6 months (Fig 1) to assess the impact of HFD on EC PGC-1α gene expression in organs, and for 12 months in EC-KO and control mice (Fig 6) before skin wound healing experiments and hindlimb ischemia surgery. (iii) *ob*/*ob* mice, which possess homozygous null mutation for the gene encoding leptin, were purchased from Charles River (Yokohama, Japan) and used at the age of 8 wk. (iv) *db*/*db* mice, which possess homozygous null mutation *($Lepr^{db}$)* for the gene encoding leptin receptor, were purchased from CLEA Japan (Tokyo, Japan) and used at the age of 10 wk as a genetic model for type 2 diabetes.

**Cell migration assay**

Transwell migration assay: Endothelial cells grown to subconfluence were detached by trypsinization, suspended in DMEM containing 0.4% FBS and applied to 8-$\mu$m-pore Transwell ($10^5$ cells/insert) pre-coated with gelatin, which was then inserted into a well containing the same media with or without mouse VEGF (10-100 ng/ml; Sigma), or sphingosine 1-phosphate (S1P) (100 nM; Enzo Life Sciences, Farmingdale, NY). The Rac1 and eNOS inhibitors were added to the cell suspension in the upper compartment. The cells were allowed to migrate across the membrane for 6 hr. The migrated cells on the lower side of the membrane were stained with Diff Quick or DAPI, and counted in 4 random fields (20X lens) under microscope.
Scratch migration assay: Confluent EC monolayer was streaked at 1-mm width with a rubber scraper. The wound edge was marked with a coverslip placed on the dish bottom. After 16 hours (for HUVECs) to 40 hours (for mouse ECs), the migrated cells beyond the edge were counted in 4 random fields (4x lens).

**Tube formation assay**

HUVECs (10,000 cells) suspended in growth medium were seeded on top of matrigel in each well of a 96-well plate. After 12-hour incubation, each well was photographed. Branching points were quantified, as described previously (Jiang et al., 2009).

**Aortic capillary sprouting assay**

As described previously (Sawada et al., 2009; Sawada et al., 2008), thoracic aorta segments (~1 mm long, 8-10 segments per aorta) were dissected from 2-3 mice per group and implanted in 0.4 ml of Matrigel (BD Bioscience, San Jose, CA). Each explant was photographed under microscope

at day 5-8. The *ex vivo* angiogenesis was determined as the area of capillary outgrowth using Image J software.

**Immuno-quantification of PGC-1α protein abundance**

One mg of protein from cellular homogenate was pre-cleared by incubation with 40 μL of control Protein A/G agarose resin to minimize non-specific binding. Five μg of anti-PGC-1α (H300) antibody (Santa Cruz) was incubated with pre-cleared lysates along with 40 μL of control Protein A/G agarose beads overnight at 4°C. Following washes of immune complexes, immunoprecipitates were collected by centrifugation, boiled in 25 μL of Laemmli sample buffer, and used for immunoblot analysis for PGC-1α using anti-PGC-1α (4C1.3) antibody (Millipore). Detection was performed using ultrasensitive horseradish peroxidase chemiluminescence (Millipore).

**Virus experiments and gene knockdown**

For PGC-1α gene transduction to HUVECs, ECFCs, and EPCs, we used a retrovirus-based system. Mouse PGC-1α cDNA cloned in MMLV vector or control empty vector was transfected into Phoenix cells using the calcium phosphate method, which then yielded PGC-1α expressing retrovirus in the supernatant. For gene knockdown experiments, we used a lentivirus-based gene transduction (The RNAi Consortium, Broad Institute, Cambridge, MA). A construct expressing short-hairpin RNA for human *ADAMTS10* (clone TRCN0000050330) or a control expressing shRNA for *GFP* cloned in pLKO.1 was transfected in HEK293T cells using lipofection with X-tremeGENE 9 (Roche, Mannheim, Germany). The supernatant containing high-titer lentivirus expressing shRNA was used to transduce HUVECs.

**Immunofluorescence**

Human ECFCs, EPCs and mouse ECs cultured on Labtek II chamber slides (Nunc) were stimulated with VEGF (100 ng/ml), S1P (100 nM) or Stromal cell-derived factor-1α (SDF-1α) (100 ng/ml) for 30 min, and fixed with 3.7% paraformaldehyde in PBS for 10 min on ice. To visualize F-actin, the cells were incubated with 1U/ml Alexa488 or Alexa546-conjugated phalloidin and DAPI (Molecular Probe) for 20 min. The fluorescent images were captured by confocal microscope (Zeiss).

**ROS measurement**

The intracellular ROS levels of cells were determined using CM-H2DCFDA (Molecular Probe). Cells were incubated with 5 uM CM-H2DCFDA for 30 min and washed with culture media. Fluorescence was read with excitation/emission filters of ~492–495/517–527 nm, as described (Jiang et al., 2009). The intracellular hydrogen peroxide level was assessed using Hyper2 biosensor(Belousov et al., 2006) that was expressed in BAECs using lentivirus-mediated transduction. Briefly, HyPer2 fluorescence was excited with 420/40 and with 500/16 band-pass excitation filters; corresponding YFP emission was acquired every 5 s for 15 min using a 535/30 bandpass emission filter. The HyPer2 ratio was quantitated in imaged cells as previously described in detail (Kalwa et al., 2012). Microscopic analysis of samples was performed using an Olympus IX81 inverted microscope in conjunction with a DSU spinning disk confocal system equipped with a Hamamatsu Orca ER cooled-CCD camera. Images were acquired using a 20X or 100X differential interference contrast oil immersion objective lens and analyzed using MetaMorph software (Universal Imaging, Downingtown, PA).

**NO measurement**

HUVECs were treated with Krebs-Ringer-Phosphate buffer containing 10 $\mu$M Diaminofluorescein-2 (DAF-2, Cayman Chemical, Ann Arbor, MI), an NO-sensitive fluorescent

dye, with or without 10 ng/ml VEGF, for 1 hour. Fluorescence was read with excitation/emission filters of 485/520 nm using OPTIMA-6 fluorescent microplate reader (BMG Labtech, Ortenberg, Germany).

**ECFCs isolation and in vivo vasculogenesis assay**

Human umbilical cord blood was obtained from the Brigham and Women's Hospital. Cord blood–derived ECFCs were obtained from the mononuclear cell (MNC) fractions. MNCs were seeded on 1% gelatin-coated tissue culture plates using endothelial basal medium (EBM-2) supplemented with SingleQuots (except for hydrocortisone) (Cambrex Bio-Science, Walkersville, MD), 20% FBS (Hyclone, Logan, UT), glutamine-penicillin-streptomycin (GPS; Invitrogen, Carlsbad, CA), and 15% autologous plasma. Colonies were allowed to grow until confluence, trypsinized, and purified using CD31-coated magnetic beads (Dynal Biotech, Brown Deer, WI). The formation of vascular networks in vivo was evaluated using a xenograft model as described (Melero-Martin et al., 2008). Mesenchymal progenitor cells (MPCs) were isolated from the mononuclear cell (MNC) fraction of a human bone marrow sample (Cambrex Bio Science, Walkersville, MD). MNCs were seeded on 1% gelatin-coated tissue culture plates using EGM-2 (except for hydrocortisone, VEGF, bFGF, and heparin), 20% FBS, 1x GPS and 15% autologous plasma, and maintained in culture using MPC-medium: EGM-2 (except for hydrocortisone, VEGF, bFGF, and heparin), 20% FBS, and 1x GPS. For xenograft experiments, a total of $1.9\times10^6$ cells was resuspended in 200 $\mu$L of ice-cold Phenol Red-free Matrigel (BD Bioscience), at a ratio of 40:60 (ECFCs:MPCs). The mixture was implanted on the back of a 6-week-old male athymic nu/nu mouse (Massachusetts General Hospital, Boston, MA) by subcutaneous injection. Implants were harvested after 7 days, fixed, sectioned and stained with Hematoxylin-Eosin. Vessel density was determined by counting luminal structures with red blood cells.

**Carotid artery injury**

Mechanical wire injury of the mouse carotid artery was performed to examine re-endothelialization. The mice were anesthetized with ketamine/xylazine prior to surgical exposure of the right carotid artery. Endothelial denudation of the common carotid artery was performed with 5 passes of an 0.14 inch guide wire which was inserted through an arteriotomy in external carotid artery. After wire removal, the external carotid artery was ligated proximal and distal to the wire insertion site, and the skin incision was closed with staples. Re-endothelialization was assessed at day 3 and 7 using the Evans blue method: following tail vein injection of 5% Evans blue dye, mice were euthanized and perfused with PBS and 10% phosphate-buffered formalin. The arteries were then be removed and opened longitudinally to expose the luminal surface for digital imaging. The re-endothelialized area (white, unstained) and non-endothelialized area (blue) were quantified using NIH Image J software. All surgeries, tissue harvests, and evaluations were done blinded to the genotype of the animals.

**Blood flow measurements**

Animal studies were approved by the MGH Subcommittee on Research Animal Care. Mice were anesthetized with an intraperitoneal injection of ketamine (80 mg/kg) and xylazine (12 mg/kg) and the right carotid artery was exposed. Carotid artery blood flow was recorded using an ultrasonic flow probe placed on the artery and sampled at 0.1 kHz using a transit-time perivascular flow meter (Transonic, MA0.5PSB and TS420, respectively). Murine electrocardiograms (ECG) were recorded using a 2-lead technique with subdermal needle electrodes (ADInstruments). Blood flow and ECG heart rate were recorded continuously in unison throughout the experiment using an analog-to-digital converter (ADC; ADInstruments, Powerlab 40/3) at a sampling rate to 100 kHz. All data was recorded and analyzed using LabChart 7 (ADInstruments, v7.1.2). For each experiment, carotid artery blood flow was

measured at baseline and then continuously thereafter. Systemic bolus administrations of acetylcholine (8 $\mu$g/kg) were delivered in a volume of 30 $\mu$L at a rate of 25 $\mu$L/sec via a tail vein catheter. Injection rate and volume were controlled by syringe pump (Harvard Apparatus, PHD 2000). After each injection, blood flow returned to baseline. Injections were spaced 3 minutes apart. Responses to acetylcholine were tested three times each in all animals.

**Vascular reactivity studies**

Vascular reactivity of carotid artery explants to carbachol was performed as described (Kanda et al., 2009). Briefly, after sacrifice (pentobarbital), left and right carotid arteries were removed from EC-PGC-1$\alpha$-Tg (Tet-On) and control mice, mounted onto glass cannulae in a pressurized system chamber (Living Systems) and maintained with perfusion (80 mmHg pressure, 37°C) in Krebs-balanced salt solution (KBSS). Vessel diameter was continuously recorded by video (IonWizard 6.2; IonOptix Corp.). Vessels were equilibrated in KBSS alone for 60 minutes before phenylephrine constriction ($10^{-5}$ M, 60 minutes). Vessel relaxation dose-response curves were generated using increasing carbachol concentrations ($10^{-8}$ – $3.10^{-6}$ M). For each experiment, carotid arteries from Tg and control mice were studied simultaneously in a 2-vessel chamber. Experiments were repeated at least 4 times in independent preparations.

**Blood pressure measurements**

To invasively measure arterial BP and total peripheral vascular resistance, transthoracic echocardiography was performed with EC-PGC-1$\alpha$-Tg mice (Tet-On) under anesthesia with sodium pentobarbital (50 mg/kg), and the right carotid artery was cannulated by the micropressure transducers (Higashikuni et al., 2010). Left ventricular stroke volume and cardiac output were calculated according to the Teichholz formula. Total peripheral vascular resistance (mmHg*min/L) was determined as mean BP divided by cardiac output. The BP of EC-KO mice was monitored by tail-cuff plethysmography (Ueda Electric Works, Tokyo, Japan).

**Wound healing assay**

Wound healing assay in vivo was performed according to a published method (Dioufa et al., 2010). After administration of anesthesia (ketamine/xylazine or Pentobarbital), mice were shaved in the back, wiped with ethanol, and wounds were made by using a biopsy punch (5 mm). To monitor wound healing, the mice were anesthetized every 2 to 3 days, and the digital pictures of wounds were acquired. Wound area measurements were conducted by ImageJ software (NIH).

**Hindlimb ischemia**

Hindlimb ischemia was performed as described previously (Sawada et al., 2008). Briefly, limb ischemia was instigated by ligation and excision of the left femoral artery. Laser Doppler perfusion image (LDPI) was taken under pentobarbital anesthesia to monitor blood flow recovery at day 0 (pre- and post-surgery), day 3, 7, 14, 21 and 28, using LDPI analyzer (Moor Instruments, Inc. DE). The LDPI intensity of the ischemic limb was normalized by that of the contralateral limb, and represented as relative blood flow of the ischemic limb. Clinical score was followed up and evaluated as the number of necrotic toes in the ischemic limb.

**Statistics**

All data are expressed as means ± standard errors of the means (SEM). One-way or two-way analysis of variance (ANOVA) followed by *post hoc* Fisher's test was used for comparison between groups. Values of $P$ of $<0.05$ were considered significant.

# Supplemental References


Belousov, V.V., Fradkov, A.F., Lukyanov, K.A., Staroverov, D.B., Shakhbazov, K.S., Terskikh, A.V., and Lukyanov, S. (2006). Genetically encoded fluorescent indicator for intracellular hydrogen peroxide. Nat Methods *3*, 281-286.

Dioufa, N., Schally, A.V., Chatzistamou, I., Moustou, E., Block, N.L., Owens, G.K., Papavassiliou, A.G., and Kiaris, H. (2010). Acceleration of wound healing by growth hormone-releasing hormone and its agonists. Proc Natl Acad Sci U S A *107*, 18611-18615.

Handschin, C., Choi, C.S., Chin, S., Kim, S., Kawamori, D., Kurpad, A.J., Neubauer, N., Hu, J., Mootha, V.K., Kim, Y.B., et al. (2007). Abnormal glucose homeostasis in skeletal muscle-specific PGC-1alpha knockout mice reveals skeletal muscle-pancreatic beta cell crosstalk. J Clin Invest *117*, 3463-3474.

Higashikuni, Y., Sainz, J., Nakamura, K., Takaoka, M., Enomoto, S., Iwata, H., Sahara, M., Tanaka, K., Koibuchi, N., Ito, S., et al. (2010). The ATP-binding cassette transporter BCRP1/ABCG2 plays a pivotal role in cardiac repair after myocardial infarction via modulation of microvascular endothelial cell survival and function. Arterioscler Thromb Vasc Biol *30*, 2128-2135.

Jiang, A., Hu, W., Meng, H., Gao, H., and Qiao, X. (2009). Loss of VLDL receptor activates retinal vascular endothelial cells and promotes angiogenesis. Invest Ophthalmol Vis Sci *50*, 844-850.

Kalwa, H., Sartoretto, J.L., Sartoretto, S.M., and Michel, T. (2012). Angiotensin-II and MARCKS: a hydrogen peroxide- and RAC1-dependent signaling pathway in vascular endothelium. J Biol Chem *287*, 29147-29158.

Kanda, T., Brown, J.D., Orasanu, G., Vogel, S., Gonzalez, F.J., Sartoretto, J., Michel, T., and Plutzky, J. (2009). PPARgamma in the endothelium regulates metabolic responses to high-fat diet in mice. J Clin Invest *119*, 110-124.

Kisanuki, Y.Y., Hammer, R.E., Miyazaki, J., Williams, S.C., Richardson, J.A., and Yanagisawa, M. (2001). Tie2-Cre transgenic mice: a new model for endothelial cell-lineage analysis in vivo. Dev Biol *230*, 230-242.

Koni, P.A., Joshi, S.K., Temann, U.A., Olson, D., Burkly, L., and Flavell, R.A. (2001). Conditional vascular cell adhesion molecule 1 deletion in mice: impaired lymphocyte migration to bone marrow. J Exp Med *193*, 741-754.

Lin, J., Wu, P.H., Tarr, P.T., Lindenberg, K.S., St-Pierre, J., Zhang, C.Y., Mootha, V.K., Jager, S., Vianna, C.R., Reznick, R.M., et al. (2004). Defects in adaptive energy metabolism with CNS-linked hyperactivity in PGC-1alpha null mice. Cell *119*, 121-135.

Masuda, H., Alev, C., Akimaru, H., Ito, R., Shizuno, T., Kobori, M., Horii, M., Ishihara, T., Isobe, K., Isozaki, M., et al. (2011). Methodological development of a clonogenic assay to determine endothelial progenitor cell potential. Circ Res *109*, 20-37.

Masuda, H., Kalka, C., Takahashi, T., Yoshida, M., Wada, M., Kobori, M., Itoh, R., Iwaguro, H., Eguchi, M., Iwami, Y., et al. (2007). Estrogen-mediated endothelial progenitor cell biology and kinetics for physiological postnatal vasculogenesis. Circ Res *101*, 598-606.

Melero-Martin, J.M., De Obaldia, M.E., Kang, S.Y., Khan, Z.A., Yuan, L., Oettgen, P., and Bischoff, J. (2008). Engineering robust and functional vascular networks in vivo with human adult and cord blood-derived progenitor cells. Circ Res *103*, 194-202.

Nakamura, T., Tsutsumi, V., Torimura, T., Naitou, M., Iwamoto, H., Masuda, H., Hashimoto, O., Koga, H., Abe, M., Ii, M., et al. (2012). Human peripheral blood CD34-positive cells enhance therapeutic regeneration of chronically injured liver in nude rats. J Cell Physiol *227*, 1538-1552.

Russell, L.K., Mansfield, C.M., Lehman, J.J., Kovacs, A., Courtois, M., Saffitz, J.E., Medeiros, D.M., Valencik, M.L., McDonald, J.A., and Kelly, D.P. (2004). Cardiac-specific induction of the transcriptional coactivator peroxisome proliferator-activated receptor gamma coactivator-1alpha promotes mitochondrial biogenesis and reversible cardiomyopathy in a developmental stage-dependent manner. Circ Res *94*, 525-533.

Sawada, N., Kim, H.H., Moskowitz, M.A., and Liao, J.K. (2009). Rac1 is a critical mediator of endothelium-derived neurotrophic activity. Sci Signal *2*, ra10.

Sawada, N., Salomone, S., Kim, H.H., Kwiatkowski, D.J., and Liao, J.K. (2008). Regulation of endothelial nitric oxide synthase and postnatal angiogenesis by Rac1. Circ Res *103*, 360-368.

Sun, J.F., Phung, T., Shiojima, I., Felske, T., Upalakalin, J.N., Feng, D., Kornaga, T., Dor, T., Dvorak, A.M., Walsh, K., et al. (2005). Microvascular patterning is controlled by fine-tuning the Akt signal. Proc Natl Acad Sci U S A *102*, 128-133.

Teng, P.I., Dichiara, M.R., Komuves, L.G., Abe, K., Quertermous, T., and Topper, J.N. (2002). Inducible and selective transgene expression in murine vascular endothelium. Physiol Genomics *11*, 99-107.